Thermal attenuation in atom-surface scattering: A useful approximation

G. Armand
Service de Physique des Atomes et des Surfaces, Centre d'Etudes Nucléaires de Saclay, 91191 Gif-sur-Yvette, France

J. R. Manson
Department of Physics and Astronomy, Clemson University, Clemson, South Carolina 29633-1911
(Received 13 April 1987)

The calculation of the specular beam intensity in atom-surface scattering as a function of crystal temperature can be achieved with good accuracy using a simple procedure presented here. This assumes the calculation of the T-matrix element for single-phonon virtual exchange and an approximate but analytical resummation allows one to include the multiphonon events. Thus the extraction of physical quantities from experimental data becomes easier, and for this purpose two simple procedures are proposed.

I. INTRODUCTION

The scattering of thermal energy atoms, particularly He atoms, is an important tool for studying surface structure and surface dynamical properties.[1] We consider here the thermal attenuation of the diffracted beam intensities which are observed when a monoenergetic atomic beam is scattered by a periodic surface. Correction for this thermal attenuation, or Debye-Waller effect, is a key question in the interpretation of experimental results. In several recent publications we have developed a calculation method and presented numerical results.[2-9] The expression obtained for the T-matrix element is a perturbation expansion where in each term one can make an expansion corresponding to the virtual exchange of 1, $2,\ldots,n$ phonons. In this way, the calculation can be made as exact as desired if one calculates a sufficient number of partial T-matrix elements, this number depending on the crystal temperature and the potential interaction. In practice, this procedure is impractical. Thus the terms corresponding to one-phonon (Refs. 2–4) and two-phonon (Ref. 5) events have been calculated exactly and a resummation procedure has been proposed[6] in order to recover the effects of the multiphonon virtual exchange.

The numerical calculations have been performed using a potential model valid for a flat surface. The anharmonicity has been introduced through the quasiharmonic approximation. The fit to the experimental data in the scattering of helium, molecular hydrogen, and neon is excellent. Using helium data we have shown that the anharmonicity on the (100) face of copper is certainly higher than in the bulk.[7]

However, the use of this calculation method to interpret experimental data is not easy. In order to facilitate this operation, several approximations have been proposed.[8,9] As we are able to compare their validity, taking as reference the results yielded by the resummation procedure, we intend in this paper to present the best approximation and to suggest a simple procedure allowing one to extract from the experimental data the relevant mean-square surface displacement and the surface anharmonicity strength.

II. POTENTIAL MODEL

The potential has been described in previous publications. It is written as

$$V=D\{\exp[-2\chi(z-u)-2\chi^2\langle\langle\mu^2\rangle\rangle]-2\exp(-\chi z)\}\ . \tag{1}$$

The repulsive part is thermally displaced in a direction normal to the surface by the displacement operator u. Its thermal average (notation $\langle\langle\ \rangle\rangle$) yields a Morse potential which has been chosen as the distorted potential for writing the T-matrix equation.

Its ability to model the real interaction between the particle and the surface has been fully discussed in preceding papers. The most important deficiency is probably the lack of exchange of momentum parallel to the surface between the particle and the surface vibrations. In fact, in the thermal attenuation of the scattered beam the phonons of low frequency are the most efficient; that is to say, those of low parallel momentum. Thus the total exchange of this quantity will be small and the potential used in this calculation can yield results which are close to results produced by a more sophisticated potential where the exchange of parallel momentum is allowed. This fact has been confirmed recently.[10]

III. THE BEST APPROXIMATION

The dimensionless T-matrix element which accounts for the total virtual exchange of one phonon can be written as[5]

$$F_1=4(A^2D)^2\left[\int_0^\infty {}_{p_i}f_p\,G(c_p,T)\,{}_pf_{p_i}\,dp+\sum_b {}_{p_i}l_b\,G(c_b,T)\,{}_bl_{p_i}\right], \tag{2}$$

with

$$G(c_q,T)=4\frac{m}{M}\int_{-\Omega_m}^{\Omega_m}\frac{\rho(\Omega)}{\Omega}\langle\langle n(\Omega)\rangle\rangle\frac{1}{c_q+\Omega+i\epsilon}d\Omega\ ,$$

where q takes on the values p and b for continuum and bound states, respectively, with $c_p=p_i^2-p^2$ and $c_b=p_i^2+\Omega_b$. T labels the crystal temperature contained in the Bose-Einstein factor $\langle\langle n(\Omega)\rangle\rangle$; m and M are, respectively, the incident-particle mass and the crystal-atom mass, $\rho(\Omega)$ the spectral density of atoms belonging to the surface unit cell, and Ω_m is the maximum crystal frequency [$\rho(\Omega)=\rho(-\Omega)$]. All the quantities are written in dimensionless form with the help of the factor $A^2=2m/\hbar\chi^2$. One has $\Omega=A^2\hbar\omega$, $\Omega_b=A^2|e_b|$, with e_b the bound-state energy and p_i the reduced normal incident-particle momentum k_i^z/χ. f and l are the following matrix elements:

$$_{p_i}f_p=\langle\phi_{p_i}|\exp(-2\chi z)|\phi_p\rangle\ ,$$

$$_{p_i}l_b=\langle\phi_{p_i}|\exp(-2\chi z)|\phi_b\rangle\ ,$$

in which ϕ_p and ϕ_b are, respectively, the eigenstates for continuum and bound states of the distorted potential. The isopotential displacement of our potential in Eq. (1) is equal to $2u$ for small values of V. In order to compensate for this effect, which is due to the subtraction of the static attractive part of the potential, the real spectral density should be multiplied by a factor $\alpha=\frac{1}{4}$.

The corresponding diagram is represented in Fig. 1(a), where the vertex represents the matrix element f or l and the straight lines are the dressed Green's operators.

The specular intensity, or more precisely, the reflection coefficient, is given by

$$R_1=\left|1-\frac{i\pi}{8p_i}F_1\right|^2\ .$$

At this stage it contains only the one-phonon effect and the result will be useful in the low-crystal-temperature domain where the two- and higher-phonon events are negligible. In order to extend the range of validity of such an expression, we sum up the contribution of bubble diagrams; that is to say, those depicting a succession of single-phonon bubbles, each of them separated by a free propagator [Fig. 1(b)]. Then if we neglect the principal value in the free propagators, the series to sum up is of a geometrical type and we get

$$F=\frac{F_1}{1+\frac{i\pi}{8p_i}F_1}\ .$$

The reflection coefficient is now given by

$$R=\left|\frac{1-\frac{i\pi}{8p_i}F_1}{1+\frac{i\pi}{8p_i}F_1}\right|^2=\frac{\left[1-\frac{\pi}{8p_i}|\mathrm{Im}F_1|\right]^2+\frac{\pi^2}{64p_i^2}(\mathrm{Re}F_1)^2}{\left[1+\frac{\pi}{8p_i}|\mathrm{Im}F_1|\right]^2+\frac{\pi^2}{64p_i^2}(\mathrm{Re}F_1)^2}\ , \tag{3}$$

where Re and Im indicate, respectively, the real and imaginary parts of F_1. In the harmonic approximation where Ω_m is independent of T, the matrix element F_1 is proportional to T in the medium- and high-temperature ranges. Then,

$$R=\frac{(1-aT)^2+bT^2}{(1+aT)^2+bT^2}\ .$$

with a and b being constants.

Obviously this approximation neglects the contribution of many diagrams. But it happens that if F_1 is calculated exactly, the reflection coefficient obtained in this way is equal within a few percent to those calculated with the complete resummation procedure. This has been numerically checked in the case of He and H_2 scattered by flat copper (100) surfaces in the temperature range 0–1300 K for He and 0–800 K for H_2, if p_i remains less than about 7. An example of such a calculation is given in Fig. 2. The parameter p_i is the only one which accounts for the incident conditions of the particle (energy and incident angle). As p_i increases beyond the value of approximately 7, the agreement between the two calculated R values

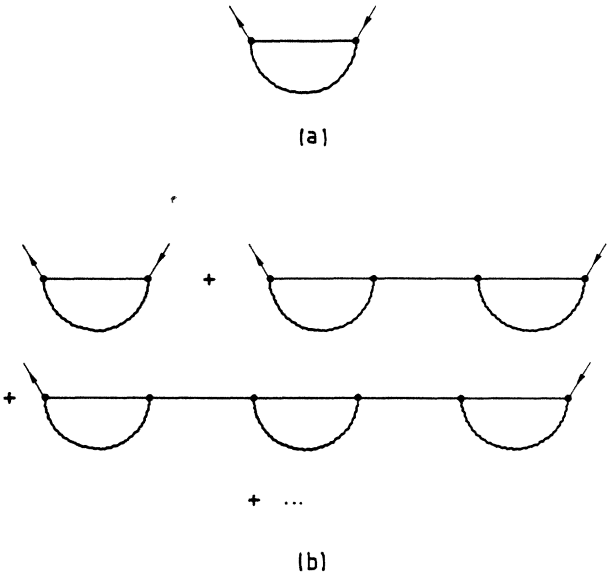

FIG. 1. (a) Diagrammatic representation of one-phonon virtual exchange. (b) Diagrams which are summed up and give expression (3).

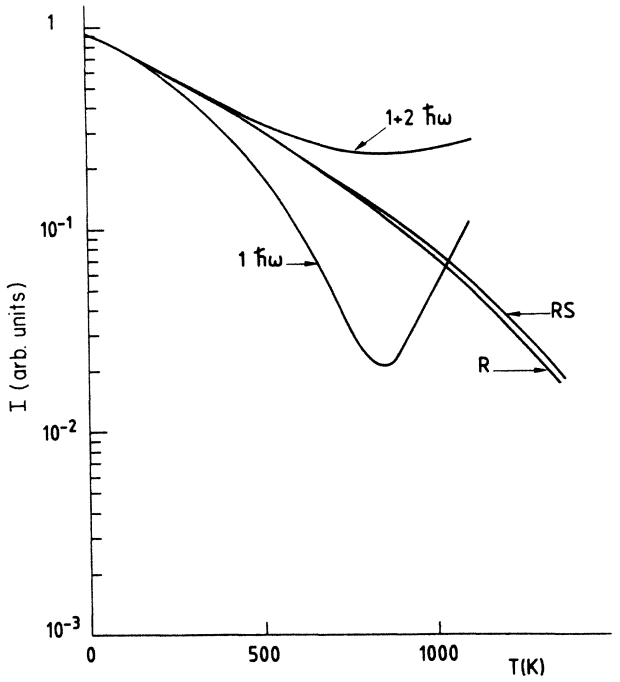

FIG. 2. Comparison of calculated intensities, with the resummation procedure (RS) and formula (3) (R). For completeness the intensity curves in case of single- and single-plus-double virtual-phonon exchange are given. $p_i = 6.52$ corresponding to He with $k_i = 11$ Å^{-1} and $\theta_i = 51.5°$; $\alpha = \frac{1}{4}$.

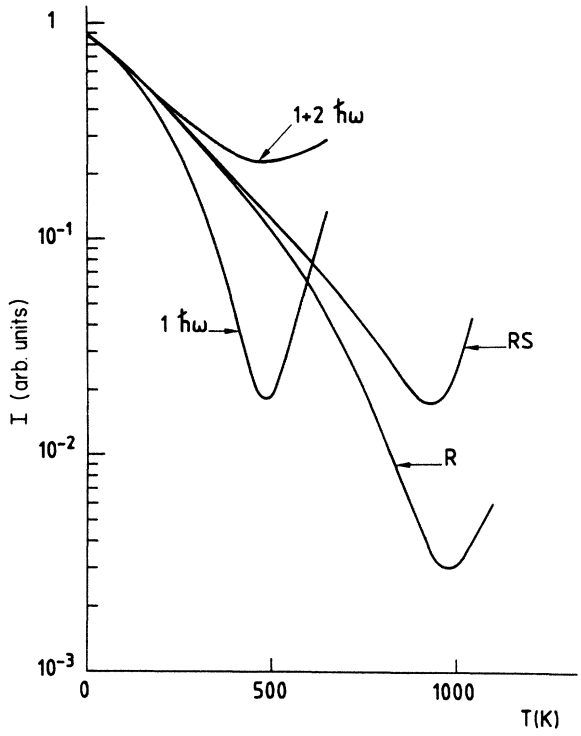

FIG. 3. Same as Fig. 2, but for $p_i = 9.905$.

is less and less good in the high-temperature domain. This is signaled by the appearance of a minimum on the $R(T)$ curves, which indicates that the multiphonon processes have not been taken into account properly (5). The calculated intensity remains good only for crystal temperatures lower than that of the minimum. For instance, with an incident helium beam of $k_i = 11$ Å^{-1} and incident angle $\theta_i = 19°$ ($p_i = 9.905$) the approximation gives correct results up to $T = 400$ K, a temperature greater than those for which the two-phonon events become non-negligible (Fig. 3).

It is not clear why this approximation gives such good results. This could be considered as an empirical rule valid for the particular potential chosen and probably also valid for other potentials. It could be used to calculate intensities of helium beams scattered by crystals other than copper. For most metals the well depth and χ values remain close to those of the helium-copper system. The spectral density shape for a noncorrugated face does not change drastically. However, for metals the Debye temperature Θ_D and the atom mass M will be different from those of copper ($\Theta_D = 350$ K for Cu). A reduction of the former quantity is accounted for by a contraction of the frequency scale and produces a decrease of R values. An augmentation in the latter quantity yields the reverse effect. Thus one can expect that the approximation proposed here will be good in the same p_i range as for copper, and in any case for crystal temperatures well below the eventual intensity minimum.

Some details about the numerical calculation of F_1 are given in Appendix A. This supposes knowledge of the spectral density relative to atoms belonging to a unit cell; that is to say, the spectral density of one atom and the correlated spectral density between nearest neighbors, next-nearest neighbors, etc., depending on the surface unit-cell shape. This calculation can be achieved by calculating the spectral density for a given point in the Brillouin zone and performing the summation with appropriate weighting factors over special points of this zone.[11] The generating coefficient method seems to be the most powerful method, but others can be used.

Once the relevant spectral density is available for an $\Omega_{\max}$ value relative to low crystal temperature, the comparison between R_1 and R gives the temperature where the one-phonon calculation becomes insufficient. Furthermore, the comparison between R and the experimental data (corrected for the unitarity defect) should exhibit a discrepancy in the medium- and high-temperature ranges if anharmonic effects are important. In order to get quantitative information on the surface anharmonicity, one can fit the experimental data for each temperature by a contraction of the frequency scale corresponding to a lower $\Omega_{\max}$ value (quasiharmonic approximation). Once $\Omega_{\max}$ is determined the calculation of $\langle\langle u^2 \rangle\rangle$ is straightforward [see Eq. (8) below].

IV. A SIMPLER APPROXIMATION

We now examine a method allowing one to extract from the experimental data the physical quantity $\langle\langle u^2 \rangle\rangle$, the mean-square displacement of the operator u in formula (1), which can be considered as the "potential mean-square displacement." This method is based on an approximation which avoids the calculation of the spectral

density and of the real part of the matrix element F_1. Consequently, the results obtained will be less precise than those yielded by the preceding method.

Neglecting the real part of F_1 one gets

$$R_I=\left[\frac{1-\frac{\pi}{8p_i}\,|\,\mathrm{Im}F_1\,|}{1+\frac{\pi}{8p_i}\,|\,\mathrm{Im}F_1\,|}\right]^2 , \tag{4}$$

or, conversely,

$$\frac{\pi}{8p_i}\,|\,\mathrm{Im}F_1\,|=\frac{1-R_I^{1/2}}{1+R_I^{1/2}} . \tag{5}$$

$|\,\mathrm{Im}F_1\,|$ is calculated from expression (2). Performing first the integration over the p variable, one has

$$|\,\mathrm{Im}F_1\,|=\alpha\pi\frac{m}{M}\int_{-\Omega_m}^{+\Omega_m}\frac{\rho(\Omega)}{\Omega}\langle\langle n(\Omega)\rangle\rangle\frac{g^2(p_i,p_\Omega)}{2p_\Omega}d\Omega ,$$

with $p_\Omega=(p_i^2+\Omega)^{1/2}$ and $g(p_i,p_\Omega)=4A^2Df(p_i,p_\Omega)$, or, with an obvious transformation,

$$\frac{\pi}{8p_i}\,|\,\mathrm{Im}F_1\,|=\alpha\frac{\pi^2}{8p_i}\frac{g^2(p_i,p_i)}{2p_i}\langle\langle U^2\rangle\rangle\chi^2 , \tag{6}$$

where $\langle\langle U^2\rangle\rangle$ is an effective mean-square displacement equal to

$$\chi^2\langle\langle U^2\rangle\rangle=\frac{m}{M}\int_{-\Omega_m}^{+\Omega_m}\frac{\rho(\Omega)}{\Omega}\langle\langle n(\Omega)\rangle\rangle\Lambda(p_i,\Omega)d\Omega \tag{7}$$

and

$$\Lambda(p_i,\Omega)=\frac{g^2(p_i,p_\Omega)}{g^2(p_i,p_i)}\frac{p_i}{p_\Omega} .$$

The analytic expression for $g(p_i,p_i)$ is known (Appendix A) and is introduced into expression (6). One gets

$$\frac{\pi}{8p_i}\,|\,\mathrm{Im}F_1\,|=\alpha\chi^2p_i^2\langle\langle U^2\rangle\rangle \times\left[1+\frac{AD^{1/2}}{p_i}\mathrm{Im}\psi(-AD^{1/2}+\tfrac{1}{2}+ip_i)\right]^2 ,$$

where ψ is the digamma function. Its imaginary part can be calculated easily (Appendix B). It is of interest to point out that $\chi^2p_i^2=(k_i^z)^2$ and that the factor in large parentheses is a well-depth correction. Its value is greater than that of the usual Beeby correction, which is equivalent in this case to replacing the square of the term in large parentheses by $1+A^2D/p_i^2$.

Now, from (5) and (7) the effective mean-square displacement $\langle\langle U^2\rangle\rangle$ could be calculated taking for R_I the actual R value; that is to say, the experimental data. For a given p_i the comparison of its variation with crystal temperature to a linear relation will give a qualitative estimation of the surface anharmonicity. However, $\langle\langle U^2\rangle\rangle$ should vary with p_i. That is to say for a given incident particle and crystal temperature, it will vary with the incident particle parameters. In fact, it is the "potential mean-square displacement"

$$\chi^2\langle\langle u^2\rangle\rangle=\frac{m}{M}\int_{-\Omega_m}^{+\Omega_m}\frac{\rho(\Omega)}{\Omega}\langle\langle n(\Omega)\rangle\rangle d\Omega , \tag{8}$$

which should be independent of p_i and is obviously the quantity which has a physical meaning.

It is therefore important to relate the known values of $\langle\langle U^2\rangle\rangle$ to $\langle\langle u^2\rangle\rangle$. With this as the object we define the ratio

$$\lambda(p_i)=\frac{\langle\langle U^2\rangle\rangle}{\langle\langle u^2\rangle\rangle} . \tag{9}$$

Since the matrix element $g(p_i,p_\Omega)$ is maximum for p_Ω very close to p_i, the quantities $\Lambda(p_i,\Omega)$ and, consequently, $\lambda(p_i)$ are less than 1. By definition this ratio is independent of the masses m or M. It has been calculated for helium scattered by a flat surface following the above procedure [from formulas (5), (7), and (8)] using the exact R value and the spectral density of four atoms belonging to (100) unit cell. For given p_i and Ω_m values it varies slightly with crystal temperature due to the influence of the real part of F_1. However, above 200 K and up to the vicinity of the temperature where the minimum on R appears, its variation is limited to within 5%. Thus, neglecting the real part of F_1 leads to the introduction of an error of just a few percent.

This ratio $\lambda(p_i)$ is dependent on the potential damping coefficient χ, the well depth D, and the Debye temperature Θ_D or, equivalently, the maximum frequency Ω_m. Figures 4 and 5 give its variation for different values of these physical quantities. Then from experimental data in an experiment where helium is scattered by a flat surface, the effective mean-square displacement $\langle\langle U^2\rangle\rangle$ can be calculated if one knows the potential parameters D and χ. Then the λ ratio and $\langle\langle u^2\rangle\rangle$ value can be estimated for different values of Θ_D. This operation should be repeated for several incident angles at a given crystal temperature. The good Θ_D value is that for which $\langle\langle u\rangle\rangle^2$ remains independent of the incident conditions.

This procedure assumes that the spectral densities of the crystal atoms are equivalent to those of the (100) face of copper. For the (100) face of other fcc metals this is probably an acceptable approximation. For a (111) face the approximation is most severe due to the fact that surface atom spectral densities are mainly dependent on surface phonons. Therefore in this case, and with this procedure, one can only obtain an estimation of the "potential mean-square displacement."

V. CONCLUSIONS

The variation of specular beam intensity with crystal temperature contains information about the dynamics of surface atoms, particularly on the surface anharmonicity. We have exposed in this paper two methods which allow one to get this information from the experimental data.

The first one supposes the knowledge of surface atom spectral densities and the calculation of the T-matrix ele-

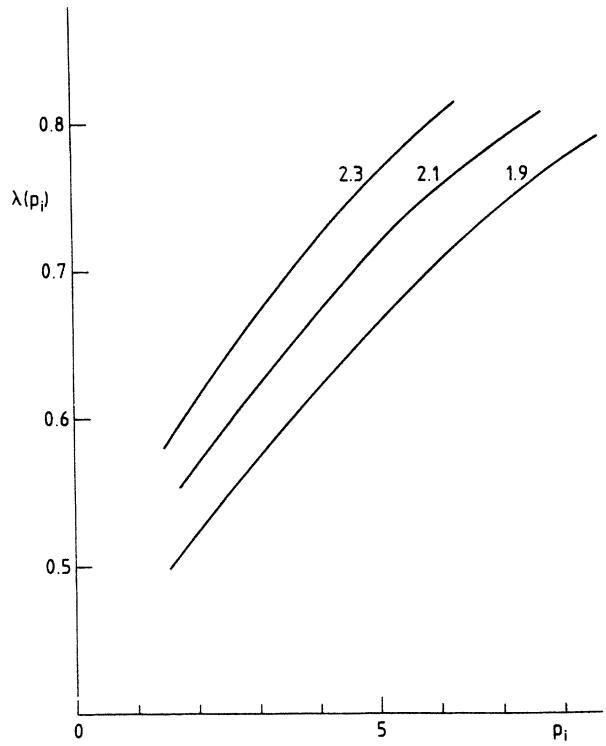

FIG. 4. Variation of the λ ratio as a function of p_i calculated with: $\Theta_D = 230$ K, $D = 6.35$ meV, spectral densities of copper (100) with $\alpha = \frac{1}{4}$. The curves are labeled by the corresponding χ values in Å^{-1}.

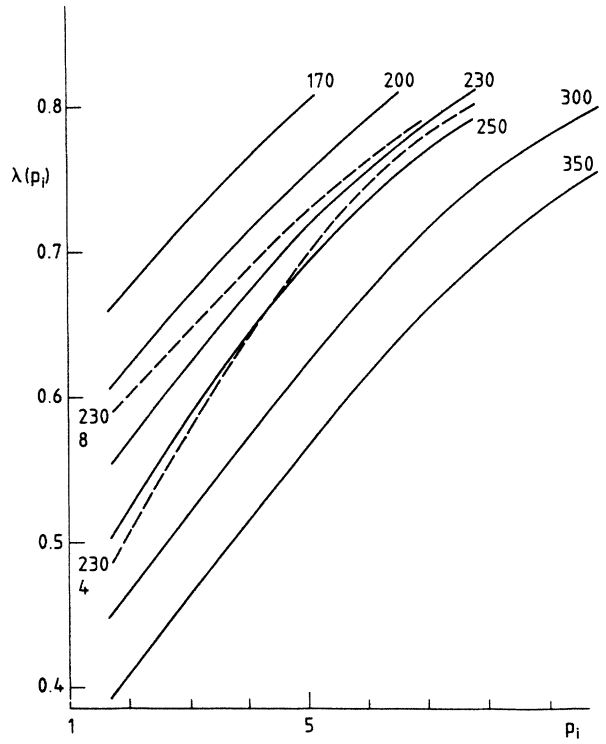

FIG. 5. Variation of the λ ratio as a function of p_i calculated with the spectral density of copper (100), $\chi = 2.1$ Å^{-1}, $\alpha = \frac{1}{4}$. Solid lines: $D = 6.35$ meV; the curves are labeled by the corresponding Θ_D value. Dashed lines: $\Theta_D = 230$ K, but D is taken to be 8 or 4 meV as marked.

ment for the single-phonon virtual exchange. In this way the errors on the deduced physical quantities are limited to a few percent.

The second method, derived from the first, avoids the calculation of spectral densities and T-matrix elements, but leads to much less precise results. It assumes that the atomic spectral densities of the surface to be studied have the same shape as those of atoms belonging to the unit cell of the (100) face of copper. Consequently, the quantities obtained are less precise, and for a face such as (111) can give only an estimation of the relevant physical quantities.

The calculated intensity in the first method, which includes the multiphonon events, is based on an infinite resummation of selected classes of terms. Its justification rests on the comparison of numerical results with a more elaborate resummation procedure. Thus its use in the case of a corrugated surface is questionable. We are not sure that it would give good intensity values even if the T-matrix element for the one-phonon virtual exchange has been calculated exactly. It may be possible that it works correctly for faces having a small corrugation. In any case, if this empirical expression is used the result should be interpreted with some care.

Throughout this paper we have assumed that the surface anharmonicity is responsible for the discrepancy between measured intensities and those calculated in the harmonic approximation in the high-crystal-temperature regime. It may happen that the surface undergoes a roughening transition, in which case the surface defects contribute to the attenuation of the specular beam intensity as surface anharmonicity does. However, in this case the influence on the peak widths should be different. In the presence of surface roughening the peak width should oscillate as a function of incident angle or incident energy with the extrema corresponding to in-phase and antiphase conditions.

APPENDIX A

The G functions are calculated for different values of the p variable and for each bound-state energy at each temperature. If the denominator does not vanish, the integration is performed directly. If it vanishes for a Ω_0 value, one has

$$G(c_q,T)=\frac{4m}{M}\left\{\frac{\rho(\Omega_0)}{\Omega_0}\langle\langle n(\Omega_0)\rangle\rangle\left[-i\pi+\mathrm{Ln}\left[\frac{\Omega_m-\Omega_0}{\Omega_m-\Omega_0}\right]\right]+\int_{-\Omega_m}^{\Omega_m}\left[\frac{\rho(\Omega)\langle\langle n(\Omega)\rangle\rangle}{\Omega}-\frac{\rho(n)\langle\langle n(\Omega_0)\rangle\rangle}{\Omega_0}\right]\frac{1}{c_q+\Omega}d\Omega\right\},$$

where q takes the values p and b as noted after Eq. (2).

For $\Omega \to 0$, $[\rho(\Omega)/\Omega]\langle\langle n(\Omega)\rangle\rangle = \lambda k T A^2$, where λ is equal to $\rho(\Omega)/\Omega^2$ in the limit of small Ω. The integration over ρ or the summation over bound states is then performed with the Morse-potential matrix elements:

$$ {}_pf_q = \frac{1}{4A^2D} \frac{[2p \sinh(2\pi p) 2q \sinh(2\pi q)]^{1/2}}{\cosh(2\pi p) - \cosh(2\pi q)} [(p^2 - q^2)C_1 + 2AD^{1/2}C_2] , $$

$$ C_1 = \left[\left| \frac{\Gamma(-AD^{1/2} + \frac{1}{2} + iq)}{\Gamma(-AD^{1/2} + \frac{1}{2} + ip)} \right| \right] + \left[\left| \frac{\Gamma(-AD^{1/2} + \frac{1}{2} + ip)}{\Gamma(-AD^{1/2} + \frac{1}{2} + iq)} \right| \right] , $$

$$ C_2 = \left[\left| \frac{\Gamma(-AD^{1/2} + \frac{1}{2} + iq)}{\Gamma(-AD^{1/2} + \frac{1}{2} + ip)} \right| \right] - \left[\left| \frac{\Gamma(-AD^{1/2} + \frac{1}{2} + ip)}{\Gamma(-AD^{1/2} + \frac{1}{2} + iq)} \right| \right] . $$

The diagonal element has the special form

$$ {}_pf_p = \frac{4p}{\pi} [p + AD^{1/2} \operatorname{Im}\psi(-AD^{1/2} + \tfrac{1}{2} + ip)] $$

and

$$ {}_pl_b = \frac{1}{4A^2D} \frac{(-1)^b}{\pi} \left[\frac{p \sinh(2\pi p)}{b!} \frac{(2AD^{1/2} - 2b - 1)}{\Gamma(2AD^{1/2} - b)} \right]^{1/2} | \Gamma(\tfrac{1}{2} - AD^{1/2} + ip) | $$

$$ \times | \Gamma(AD^{1/2} + \tfrac{1}{2} + ip) |^2 [(AD^{1/2} - b - \tfrac{1}{2})^2 + p^2 + 2AD^{1/2}] , $$

where Γ is the gamma function.

APPENDIX B

In the absence of a more convenient algorithm, one can calculate the imaginary part of the digamma function in the following way, with $z = x + iy$,

$$ \operatorname{Im}\psi(z) = y \sum_{n=0}^{\infty} \frac{1}{(x+n)^2 + y^2} , $$

or by taking the imaginary part of the asymptotic expansion,

$$ \psi(z) \sim \operatorname{Ln}(z) - \frac{1}{2z} - \frac{1}{12z^2} + \frac{1}{120z^4} - \frac{1}{252z^6} + \cdots . $$

[1]For recent reviews, see J. A. Barker and D. J. Auerbach, Surf. Sci. Rep. **4**, 1 (1984); T. Engel and K. H. Rieder, in *Structural Studies of Surfaces,* Vol. 91 of *Springer Tracts in Modern Physics,* edited by G. Höhler (Springer, New York, 1986); G. Boato and P. Cantini, Adv. Electron. Electron Phys. **60**, 65 (1983).

[2]G. Armand and J. R. Manson, Phys. Rev. Lett. **53**, 112 (1986).

[3]G. Armand and J. R. Manson, in *Dynamics on Surfaces,* edited by Bernard Pullman (Reidel, Dordrecht, 1984), Vol. 17, p. 59.

[4]C. S. Jayanthi, G. Armand, and J. R. Manson, Surf. Sci. **154**, L247 (1985).

[5]G. Armand, J. R. Manson, and C. S. Jayanthi, J. Phys. (Paris) **47**, 1357 (1986).

[6]G. Armand, J. R. Manson, and C. S. Jayanthi, Phys. Rev. B **34**, 6627 (1986).

[7]G. Armand, D. Gorse, J. Lapujoulade, and J. R. Manson, Europhys. Lett. **3**, 1113 (1987).

[8]J. R. Manson and G. Armand, Surf. Sci. **184**, 511 (1987).

[9]J. R. Manson and G. Armand (unpublished).

[10]J. Idiodi, V. Bortolani, A. Franchini, G. Santoro, and V. Celli, Phys. Rev. B **35**, 6209 (1987).

[11]G. Armand, J. Phys. (Paris) **38**, 989 (1977).